Increased *App* Expression in a Mouse Model of Down's Syndrome Disrupts NGF Transport and Causes Cholinergic Neuron Degeneration

Ahmad Salehi,[1,9,*] Jean-Dominique Delcroix,[1,9,10] Pavel V. Belichenko,[1] Ke Zhan,[1] Chengbiao Wu,[1] Janice S. Valletta,[1] Ryoko Takimoto-Kimura,[1] Alexander M. Kleschevnikov,[1] Kumar Sambamurti,[2] Peter P. Chung,[2] Weiming Xia,[3] Angela Villar,[4] William A. Campbell,[3] Laura Shapiro Kulnane,[5] Ralph A. Nixon,[6] Bruce T. Lamb,[5] Charles J. Epstein,[4] Gorazd B. Stokin,[7] Lawrence S.B. Goldstein,[7] and William C. Mobley[1,8]

[1] Department of Neurology and Neurological Sciences
Stanford University
Stanford, California 94305
[2] Center on Aging
Medical University of South Carolina
Charleston, South Carolina 29425
[3] Department of Neurology
Harvard Medical School
Boston, Massachusetts 02115
[4] Department of Pediatrics
University of California, San Francisco
San Francisco, California 94143
[5] Department of Genetics
Case Western Reserve University
Cleveland, Ohio 44195
[6] Center for Dementia Research
Nathan Kline Institute
Orangeburg, New York 10962
[7] Department of Cellular and Molecular Medicine
University of California, San Diego
La Jolla, California 92093
[8] Neuroscience Institute at Stanford
Stanford University School of Medicine
Stanford, California 94305

Summary

Degeneration of basal forebrain cholinergic neurons (BFCNs) contributes to cognitive dysfunction in Alzheimer's disease (AD) and Down's syndrome (DS). We used Ts65Dn and Ts1Cje mouse models of DS to show that the increased dose of the amyloid precursor protein gene, *App*, acts to markedly decrease NGF retrograde transport and cause degeneration of BFCNs. NGF transport was also decreased in mice expressing wild-type human APP or a familial AD-linked mutant APP; while significant, the decreases were less marked and there was no evident degeneration of BFCNs. Because of evidence suggesting that the NGF transport defect was intra-axonal, we explored within cholinergic axons the status of early endosomes (EEs). NGF-containing EEs were enlarged in Ts65Dn mice and their App content was increased. Our study thus provides evidence for a pathogenic mechanism for DS in which increased expression of App, in the context of trisomy, causes abnormal transport of NGF and cholinergic neurodegeneration.

Introduction

Alzheimer's disease (AD) is a dementing disorder that features the dysfunction and degeneration of specific neuronal populations (Cummings, 2004). Virtually all elderly people with Down's syndrome (DS), trisomy 21, show neuropathological features of AD (Wisniewski et al., 1985) and many show cognitive decline (Lai and Williams, 1989). Although the pathogenesis of DS-related neurodegeneration is poorly defined, the presence of one extra copy of one or more normal genes or regulatory sequences on chromosome 21 must be responsible. Establishing links between overexpression of these genes and AD-related phenotypes in DS will inform the pathogenesis of DS and AD.

Atrophy and loss of basal forebrain cholinergic neurons (BFCNs), a phenotype seen in AD, DS (Mann et al., 1985; Whitehouse et al., 1981), and several other neurodegenerative disorders (see Salehi et al., 1994), likely contributes to cognitive decline (Auld et al., 2002) but is poorly understood. To elucidate pathogenesis, we examined BFCN degeneration in Ts65Dn mice which are segmentally trisomic for mouse chromosome 16 (Davisson et al., 1990) and show features of DS (Belichenko et al., 2004; Cooper et al., 2001; Kleschevnikov et al., 2004). The trisomic segment contains about 140 genes with homologs on human chromosome 21 in a region associated with many DS abnormalities (Korenberg et al., 1994). The Ts65Dn mouse shows age-related atrophy and loss of BFCNs in the medial septal nucleus (MSN) as measured using immunostaining for either $p75^{NTR}$ ($p75^{NTR}$-Ir) or choline acetyltransferase (ChAT-Ir) (Cooper et al., 2001; Holtzman et al., 1996; Seo and Isacson, 2005). $p75^{NTR}$ has been extensively used to characterize these neurons (Jaffar et al., 2001). On the basis of earlier findings, we postulated that degeneration is due to the demonstrated failure of retrograde transport of nerve growth factor (NGF). NGF is a target-derived neurotrophic factor that acts through its specific receptors, TrkA and $p75^{NTR}$, to enhance the survival, differentiation, and maintenance of specific neurons of the peripheral and central nervous systems (Ye et al., 2003), including BFCNs (Sofroniew et al., 2001). In mature neurons, NGF signaling regulates expression of genes important for neuronal phenotype and cell size. The source of NGF for BFCNs in the MSN is the hippocampus; NGF produced in hippocampus binds to receptors on BFCN axons and, following endocytosis, is retrogradely transported to cell bodies (Sofroniew et al., 2001). Speaking to the importance of NGF for mature BFCNs, transgenic (Tg) mice that produce antibodies to NGF show severe age-related BFCN degeneration (Capsoni et al., 2000). Of note, we showed that the decrease in the number of BFCNs in Ts65Dn mice was not due to the death of these neurons, but rather to the downregulation of $p75^{NTR}$ gene expression, which

*Correspondence: asalehi@stanford.edu
[9] These authors contributed equally to this work.
[10] Present address: European Brain Research Institute, Rita Levi-Montalcini Foundation, 00143 Rome, Italy.

is regulated by NGF signaling (Gage et al., 1989). Indeed, bypassing the NGF transport defect through delivery of NGF to cell bodies by intracerebroventricular injection reversed deficits in BFCNs (Cooper et al., 2001). Herein, we provide evidence of a role for increased *App* gene dose and expression in causing the defect in NGF transport and the degeneration of BFCNs in the Ts65Dn mouse.

Results

Examining NGF Transport and BFCNs in Mouse Models of DS

To explore the mechanism of decreased NGF transport and its significance for degeneration of BFCNs, we used genetic models of DS: (1) Ts65Dn mice segmentally trisomic for chromosome 16; (2) Ts1Cje mice (Sago et al., 1998) segmentally trisomic for ~100 of the 140 genes present in Ts65Dn; and (3) Ts65Dn mice in which the third copy of *App* was deleted. To examine retrograde transport of NGF in BFCNs, we injected radiolabeled NGF into the hippocampus of control (2N = diploid) and Ts65Dn mice and measured radioactivity in septum 12 hr later. Transport was severely reduced in Ts65Dn mice relative to the controls (Figure 1A). Measurements at regular intervals for 24 hr after injection showed markedly decreased transport, indicating that the decrease was not due to a delay in transport (data not shown). In contrast, NGF transport was much more robust in Ts1Cje mice—about 6-fold that seen in the Ts65Dn mice and about 70% of that seen in 2N controls (Figure 1A).

Consistent with decreased retrograde transport of endogenous NGF, NGF protein levels were significantly increased in the hippocampus of Ts65Dn mice (Cooper et al., 2001) without an increase in NGF mRNA in hippocampus (Ts65Dn/2N = 0.82 ± 0.27, n = 5, p = 0.51). In addition, there was a moderate decrease in NGF in the septum, which due to technical limitations did not reach statistical significance. In accord with the improvement in NGF transport in Ts1Cje mice, the amount of NGF was not different from 2N mice in either hippocampus ([ng/g tissue (mean ± SEM)]; 2N = 3.25 ± 0.19, n = 4; Ts1Cje = 3.85 ± 0.25, n = 4; p > 0.5) or septum ([2N = 1.95 ± 0.25, n = 4; Ts1Cje = 2.46 ± 0.36, n = 4]; p > 0.5). Thus, NGF transport was little affected in Ts1Cje mouse.

If, as postulated, failed NGF transport was responsible for the degeneration of BFCNs in Ts65Dn mice, we reasoned that the improvement in NGF transport in Ts1Cje mice would be attended by improvement in the status of BFCNs. Examining elderly mice, in which changes in BFCNs in Ts65Dn mice are most evident, in Ts1Cje mice we found no significant difference with respect to 2N mice in the number or mean cell size of $p75^{NTR}$-Ir BFCNs. In contrast, the changes in Ts65Dn mice could be reconfirmed (Figures 1B and 1C). Extending these findings by examining another marker for BFCNs, we used an antibody to TrkA, which selectively marks BFCNs in the MSN (Yeo et al., 1997). There was a significant reduction in the number and size of TrkA-Ir neurons in Ts65Dn as compared with 2N mice. By contrast, in Ts1Cje mice there was no significant difference in number; while a change in size was registered, the deviation from 2N mice was significantly less than for Ts65Dn mice (Figures 2A and 2B). These data provide additional support for the assertion that disrupted NGF transport is linked to BFCN degeneration in models of DS.

Examining BFCN Axons in Mouse Models of DS

In an earlier study, we detected changes in BFCN axons in Ts65Dn mice, the most interesting of which was a significant change in the distribution of $p75^{NTR}$ immunostaining within the dentate gyrus (DG) (Cooper et al., 2001). To investigate if Ts1Cje mice also escaped this phenotype, we reevaluated in all three genotypes the distribution of BFCN axons by examining the optical density (OD) of $p75^{NTR}$ immunostaining. First, we detected no significant differences in the average OD for either hippocampus or DG (see Table S1A in the Supplemental Data); nor were there changes in the thickness of the dentate granule cell (DGC) layer or molecular layer (ML). We then mapped the pattern of $p75^{NTR}$ immunostaining in the inferior blade of the DG, from the DGC layer to the outer ML in mice of all three genotypes. In accord with an earlier report (Cooper et al., 2001), there was a change in Ts65Dn mice (Figure 1D and Figure S1 in the Supplemental Data), with an increase in intensity in the inner aspect of the ML and a decrease in more superficial aspects. Given that the overall level of $p75^{NTR}$-Ir was unchanged in DG, the findings suggest that cholinergic terminals are distributed differently within the ML in aged Ts65Dn mice. In contrast to the findings in Ts65Dn mice, the pattern of immunostaining in the DG of Ts1Cje mice was virtually identical to that of 2N mice. Thus, as for the cell bodies of BFCNs, the abnormal axonal phenotype detected in Ts65Dn was absent in Ts1Cje mice.

Increased Gene Dose and Expression for *App* Plays a Conspicuous Role in Failed NGF Transport and BFCN Degeneration in Mouse Models of DS

Because Ts65Dn and Ts1Cje mice differed with respect to NGF transport and the status of BFCNs, this suggested that increased dose of a gene(s) present in Ts65Dn, but not in Ts1Cje, was responsible. One candidate is the amyloid precursor protein (*App*) gene, the mouse ortholog of human *APP*, which is present in three copies in Ts65Dn but in only two copies in Ts1Cje (Gardiner et al., 2003). Mouse *App* is highly orthologous to human *APP* at the nucleotide and protein levels (Yamada et al., 1989) and both the mouse and human genes are widely expressed in the brain (Golde et al., 1990). In addition, recent studies have implicated APP in axon structure and function (Stokin et al., 2005). To test whether increased *App* dose disrupts NGF transport, we bred Ts65Dn females with male mice hemizygous for *App* to produce litters containing: 2N mice with two copies of *App* (2N:$App^{+/+}$); 2N mice with one copy of *App* (2N:$App^{+/-}$); Ts65Dn mice with three copies of *App* (Ts65Dn:$App^{+/+/+}$); and Ts65Dn mice with two copies of *App* (Ts65Dn:$App^{+/+/-}$). When examining NGF transport, as expected, Ts65Dn:$App^{+/+/+}$ mice showed a severe defect, achieving only ~4% of the levels seen in 2N mice (Figure 1E). Remarkably, Ts65Dn:$App^{+/+/-}$ mice achieved levels nearly 56% of those in 2N mice. Thus, deleting one copy of *App* markedly increased NGF transport, restoring it to a level similar to that in

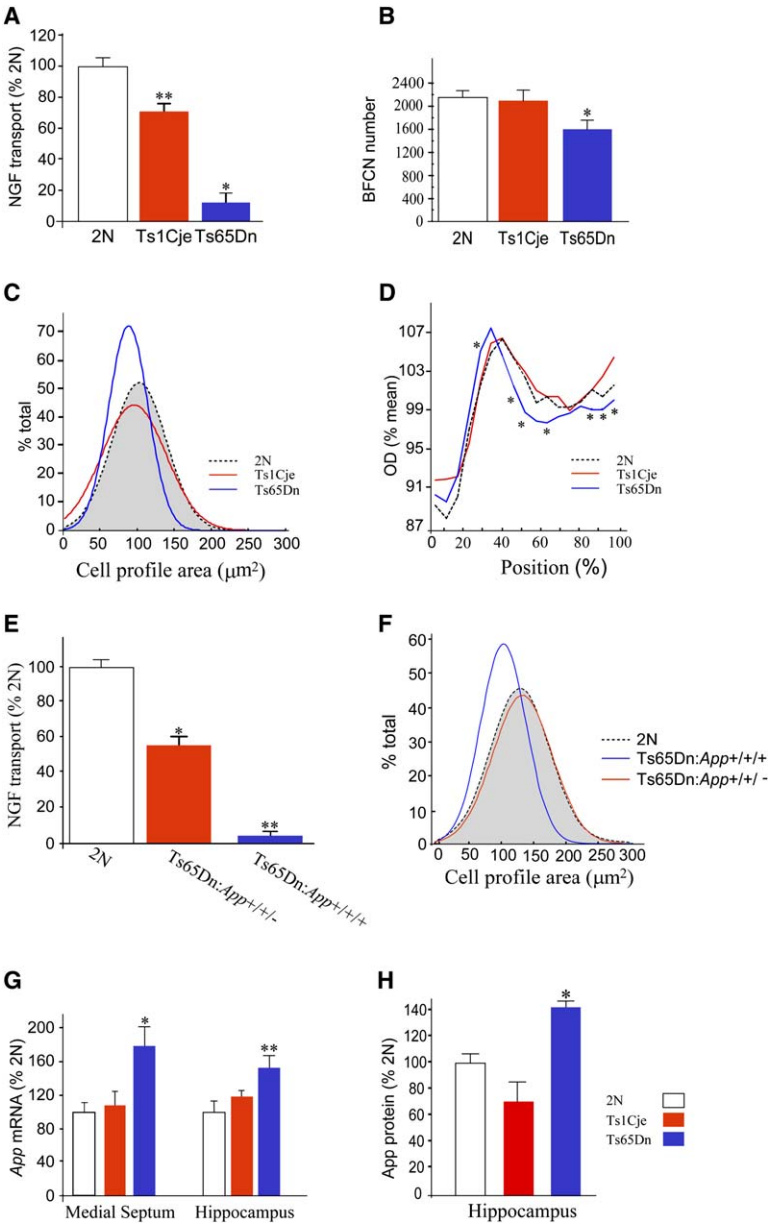

Figure 1. NGF Transport and App in Trisomic Mice

(A) Ts65Dn mice exhibited a marked decrease in NGF transport (12.6% ± 2.7% of 2N controls, n = 5, *p < 0.0001). Note that NGF transport was also markedly decreased in Ts65Dn mice at age 3 months (not shown). NGF transport was much greater in Ts1Cje mice (71.0% ± 5.1% of 2N controls, n = 5, **p = 0.0016) relative to Ts65Dn mice (p < 0.0001).

(B) The number of $p75^{NTR}$-Ir BFCNs in Ts65Dn mice (1601 ± 158, n = 5) was significantly lower than in 2N mice (2150 ± 119, n = 10, *p = 0.021). In contrast, there was no significant difference in BFCN number between Ts1Cje (2096 ± 183, n = 6, p > 0.7) and 2N controls.

(C) The frequency distribution of BFCN cell profile areas in 2N, Ts65Dn, and Ts1Cje mice. Note that the curve for Ts1Cje mice approximates that for 2N mice. In contrast, the cell profile areas of BFCNs in Ts65Dn mice (88.37 ± 0.65 μm^2, n = 5) were significantly smaller than in 2N mice (103.41 ± 4, n = 10, p = 0.007). There was no significant difference in the cell profile areas for Ts1Cje (98.3 ± 8, n = 6) and 2N mice (p > 0.6).

(D) The pattern of $p75^{NTR}$ immunostaining in the inferior blade of the DG. The normalized OD value is plotted for a line that begins from the DGC layer and extends to the outer one-third of the ML. The patterns for Ts65Dn and 2N differed significantly (significant differences marked by [*]). There was no significant difference between Ts1Cje and 2N mice.

(E) As expected, NGF transport was markedly reduced in Ts65Dn:$App^{+/+/+}$ mice as compared to controls (4.3% ± 2.3%, n = 3, **; p < 0.0001). However, transport increased in Ts65Dn:$App^{+/+/-}$ mice to 56.2% ± 4.5% (n = 3) of that in 2N mice, a highly significant change (*p = 0.0005).

(F) The BFCN atrophy in Ts65Dn:$App^{+/+/+}$ mice was not present in Ts65Dn:$App^{+/+/-}$ mice. Comparing the frequency distribution of BFCN cell profile areas, there was a significant difference (p = 0.045) between Ts65Dn:$App^{+/+/+}$ and Ts65Dn:$App^{+/+/-}$. There was also a significant difference in the absolute values for cell profile areas between Ts65Dn:$App^{+/+/+}$ (103.37 ± 5 μm^2, n = 6) and 2N mice (116.9 ± 5 μm^2, n = 5, p = 0.044), but not between 2N mice and Ts65Dn:$App^{+/+/-}$ mice (128.28 ± 0.9 μm^2, n = 2, p = 0.245).

(G) In Ts65Dn mice, but not in Ts1Cje mice, *App* mRNA levels were increased in the MSN (2N = 100.0% ± 10.8%, n = 5; Ts65Dn = 179.33% ± 22.3%, n = 5; Ts1Cje = 108.19% ± 16.2%, n = 5; 2N versus Ts65Dn, *p = 0.028; 2N versus Ts1Cje, p = 0.916) and hippocampus (2N = 100.0% ± 13.1%, n = 5; Ts65Dn = 152.89 ± 13.6, n = 4; Ts1Cje = 118.85% ± 6.5%, n = 5; 2N versus Ts65Dn, **p = 0.027; 2N versus Ts1Cje, p = 0.174).

(H) Increased levels of *App* mRNA were reflected in increased levels of App protein. The levels of FL-App in the hippocampus of Ts1Cje mice did not differ significantly from that of 2N mice (2N = 100.0% ± 8%, n = 4; Ts1Cje = 70.7 ± 8, n = 4; p = 0.155). However, there was a significant increase in the levels of FL-App in Ts65Dn mice (2N = 100.0% ± 4.5%, n = 4; Ts65Dn = 143.8 ± 4.1%, n = 4; 2N versus Ts65Dn, *p = 0.0004). Error bars = SEM.

Ts1Cje mice. That the defect in NGF transport was not fully prevented in the Ts1Cje or the Ts65Dn:$App^{+/+/-}$ mice is evidence that other genes in the trisomic segment must contribute. We next determined whether deleting the extra copy of *App* influenced the size of BFCNs. As shown (Figure 1F), while the area of BFCN cell bodies in Ts65Dn:$App^{+/+/+}$ was markedly reduced, in Ts65Dn:$App^{+/+/-}$ mice it was indistinguishable from 2N mice. These findings provide compelling evidence that increased gene dose for *App* contributes significantly to the disruption in NGF transport and atrophy of BFCNs in Ts65Dn mice.

Increased gene expression was the most likely explanation for the demonstrated effects of *App* gene dose. We first confirmed that *App* mRNA and full-length App (FL-App) protein levels are increased in Ts65Dn but not Ts1Cje mice (Figures 1G and 1H). In addition, as predicted by genotype, Ts65Dn:$App^{+/+/+}$ mice exhibited significantly increased levels of FL-App relative to the 2N controls (Table S2). We conclude that increased

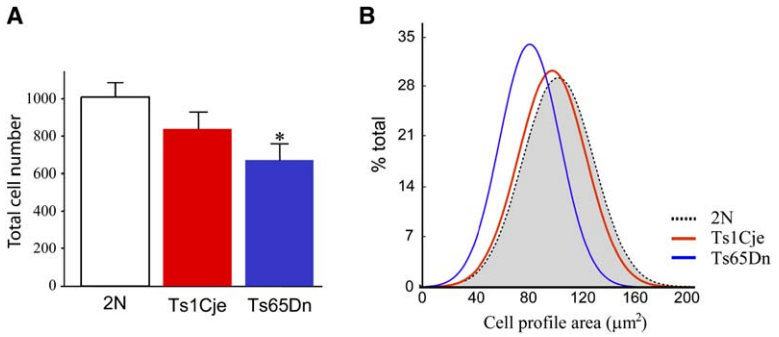

Figure 2. TrkA Expression in BFCNs of Trisomic Mice

Stereological estimation of the total number (A) and cell profile area (B) of TrkA-Ir neurons in the MSN of Ts65Dn, Ts1Cje, and their 2N controls. There was a significant reduction in the number of TrkA-Ir neurons in Ts65Dn mice compared with 2N mice (2N = 1015.21 ± 76.73, n = 11, Ts65Dn = 677.67 ± 85.64, n = 5, *p = 0.015). However, no significant reduction was found in the total number of TrkA-Ir cells in the MSN of Ts1Cje mice (Ts1Cje = 844.42 ± 89.37, n = 6, p = 0.298). The cell profile area of TrkA-Ir cells was as follows: 2N (119.39 ± 7.25 μm^2), Ts1Cje (102.74 ± 1.7 μm^2), and Ts65Dn (86.67 ± 2.69 μm^2) mice; (2N versus Ts65Dn, p = 0.0072; 2N versus Ts1Cje, p = 0.02; and Ts1Cje versus Ts65Dn, p = 0.01). The frequency distribution indicates that while the distribution of profile area was shifted to lower values in Ts65Dn mice, this was not the case for Ts1Cje mice.
Error bars = SEM.

App gene dose was reflected in increased levels of both the mRNA and protein.

Decreased NGF Transport in Mice Transgenic for Wild-Type or Mutant Human *APP*

To examine further a role for increased *APP* expression on NGF retrograde transport and BFCNs, we examined the following: (1) mice Tg for wild-type (wt) human *APP;* (2) mice Tg for a mutant of human *APP, APP_{Swe}*, known to cause Swedish familial AD (FAD); (3) mice Tg for a mutant presenilin 1 ($PS1_{A246E}$) that causes FAD; and (4) mice Tg for both APP_{Swe} and $PS1_{A246E}$. In mice Tg for a yeast artificial chromosome (YAC) containing the human wt *APP* gene (Lamb et al., 1993), the pattern of expression of the transgene is similar to that of mouse *App*, and the total (i.e., Tg plus endogenous) mRNA and protein levels approximate those found in DS and in the Ts65Dn mouse (Lamb et al., 1993). Western blot studies on brain of wt *APP* mice showed an ~70% increase, as compared to non-Tg controls, in total APP and in APP C-terminal fragments (App-CTF). The same increase was registered for the release of the Aβ peptide from cultured cortical neurons (Lamb et al., 1997). We found that NGF transport was modestly but significantly decreased in Tg mice compared to their non-Tg littermates (Figure 3A). Thus, increased expression of *APP* alone exerts a conspicuous effect on NGF retrograde transport.

To confirm a role for increased *APP* expression, we examined a mouse model of AD in which there is increased expression of an *APP* transgene bearing a mutation that causes FAD. In APP_{Swe} mice the *App* gene has been modified to encode the human sequence for the Aβ domain together with the mutations linked to Swedish FAD (K595N, M596L) (Borchelt et al., 1997). Full-length APP is increased about 2-fold over the level of endogenous mouse App and APP-CTFs are increased by at least this amount (Borchelt et al., 1996; Jankowsky et al., 2004). NGF transport was significantly decreased, achieving only 62% of that seen in non-Tg controls (Figure 3B). Decreased NGF transport could be due to a decrease in the number of BFCNs, decreased NGF binding to its receptors on the axons of these neurons, or decreased internalization of receptor-bound NGF. Because in comparing APP_{Swe} Tg mice and non-Tg controls we detected no significant differences in any of these parameters (Figures 3C–3F), the findings point to an intracellular locus for the NGF transport defect in APP_{Swe} BFCNs axons, as was seen in Ts65Dn mice (Delcroix et al., 2004).

Mutations in *PS1* modify APP processing (Price and Sisodia, 1998). In mice Tg for both APP_{Swe} and mutant human $PS1_{A246E}$, the increase in FL-APP is equivalent to that in APP_{Swe} mice—i.e., increased ~2-fold (Borchelt et al., 1997). We found that NGF transport was more compromised in the doubly Tg mice than in those harboring only the APP_{Swe} transgene; transport was reduced to ~40% of control levels (Figure 3B; $p < 0.05$). As in APP_{Swe} mice, the transport defect in doubly Tg mice was not accompanied by significant decreases in the size or number of BFCNs, in NGF receptor binding, or in NGF internalization (Figures 3E and 3F). The failure to register a change in BFCN size or number in these mice differentiates them from Ts65Dn mice and raises the possibility that only with more severe changes in NGF transport do BFCNs become atrophic and lose immunoreactivity for $p75^{NTR}$.

Studies to Elucidate the Mechanism by which Increased *App* Expression Disrupts NGF Transport

To begin to elucidate the cellular mechanism by which *App* overexpression compromises transport, we asked which product(s) of *App* gene expression is responsible. Evidence against a role for Aβ in the Ts65Dn mouse is that there is no increase in the level of either Aβ40 or Aβ42 in the whole brain or the hippocampus (Table S3). These findings directed our attention to FL-App and its other processed products. We noted with interest recent findings suggesting that increased levels of FL-App and/or one or more of its transmembrane, C-terminal-containing products could play a role in modifying axonal structure and function (Gunawardena and Goldstein, 2001). Indeed, these findings point to both axonal pathology in cholinergic neurons that overexpress *APP* and an effect on severity of gene dose for a motor protein, kinesin 1 (Stokin et al., 2005). We examined FL-App and transmembrane C-terminally intact App products, comparing the levels in Ts65Dn, Ts1Cje, and 2N mice. In Ts65Dn, but not in Ts1Cje, the levels of both the FL-App and App-CTFs—i.e., C-83 plus C-99—were increased in hippocampus roughly in proportion to gene dose (Figures 4C and 4D). When examined with respect to NGF transport, increased FL-App was associated

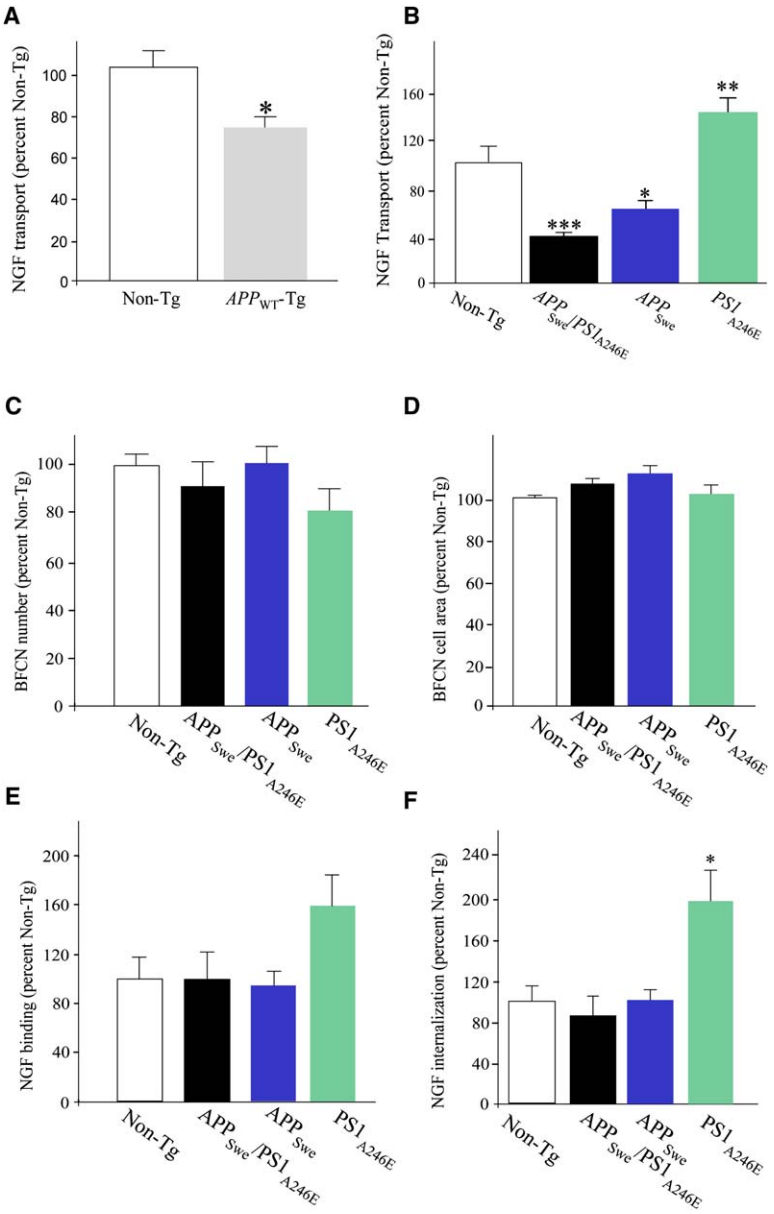

Figure 3. NGF Transport, Binding, and Internalization in *APP* Tg Mice

(A) Mice that expressed wt human *APP* at levels comparable to Down's syndrome showed a modest but significant reduction in NGF transport to 74.2% ± 7.4% (n = 4, *p = 0.002) of that of non-Tg controls.

(B) In comparison with non-Tg mice, elderly mice (age 19–20 months) overexpressing APP_{Swe} or both APP_{Swe} and $PS1_{A246E}$ showed significantly lower values for NGF transport (62.0% ± 5.7%, n = 5, *p = 0.029; and 41.35% ± 1.12%, n = 3, ***p = 0.005, respectively). The amount of NGF transported in $PS1_{A246E}$ mice was significantly greater than that in $APP_{Swe}/PS1_{A246E}$ mice (**p = 0.01).

(C) There was no difference in the number of $p75^{NTR}$-Ir neurons between non-Tg mice and the singly or doubly Tg mice. BFCN number: Non-Tg (1715 ± 79, n = 5), $APP_{Swe}/PS1_{A246E}$ (1567 ± 176, n = 6), APP_{Swe} (1731 ± 118, n = 6), $PS1_{A246E}$ (1391 ± 158, n = 5).

(D) Nor was there a difference in cell profile areas with respect to non-Tg mice. Cell profile area: Non-Tg (84.66 ± 2.3 μm^2), $APP_{Swe}/PS1_{A246E}$ (90.57 ± 2.8 μm^2), APP_{Swe} (94.86 ± 5.0 μm^2), and $PS1_{A246E}$ (86.02 ± 1.4 μm^2).

(E) There was no significant difference in the amount of NGF binding between the non-Tg controls and any of the Tg mice (Kruskal-Wallis test: p = 0.1603), although there was a definite trend toward increased binding to synaptosomes from $PS1_{A246E}$. The data report the results of the following number of determinations (non-Tg = 6, APP_{Swe} = 6, $APP_{Swe}/PS1_{A246E}$ = 8, $PS1_{A246E}$ = 8).

(F) A significant difference in NGF internalization was found between the four groups (p = 0.0116). This was due to a significant increase in NGF internalization in $PS1_{A246E}$ mice (Non-Tg versus $PS1_{A246E}$, *p = 0.014). This increase was correlated with increased NGF transport compared to non-Tg controls (141.58% ± 10.9%, n = 5, p = 0.040,) (see [B]).

Error bars = SEM.

with decreased NGF transport, but no significant linear correlation was evident across genotypes (r = −0.7582, p = 0.452) (Figure 4C). NGF transport was correlated with the concentration of App-CTFs (r = −0.999, p = 0.007). Increased levels of FL-App and CTFs were uniformly detected in trisomic mice (Table S2). To investigate if the increases in FL-App and App-CTFs in Ts65Dn mice were present in axonal terminals, we carried out studies on hippocampal synaptosomes and found increased levels for both FL-App and App-CTFs (Figures 4A and 4B). These data raise the possibility that increases in FL-App and other transmembrane Apps, including App-CTFs, negatively influence NGF transport.

One lead for elucidating the mechanism of disrupted NGF transport comes from recent studies suggesting that *App* overexpression causes the enlargement of early endosomes (EEs) in Ts65Dn BFCNs. Increased EE size is a pathological signature also seen in DS and AD (Cataldo et al., 2003). The finding can be envisioned as having a role in compromising NGF transport: endocytosis of NGF carries it to EE, retrograde transport of NGF occurs within EEs (Delcroix et al., 2003), and enlarged EEs may be transported ineffectively (Carter and Sorkin, 1998; Seet and Hong, 2001). To ask if increased App expression was registered within EEs, we used confocal immunostaining. Vesicular acetylcholine transporter (VAChT) immunoreactivity was used to mark BFCN axons in hippocampus and Rab5b immunostaining marked EEs (Figures 5 and 6). We saw that (1) cholinergic terminals are enlarged in Ts65Dn mice (Figure 6Ba); (2) cholinergic terminals of both 2N and Ts65Dn mice contain EEs (Figures 5Aa–5Ad); (3) cholinergic terminals also contain App, detected using antibodies to either the App N terminus (Figures 5Ae–5Ah and Figures 6Aa–6Ah), the C terminus (Figures 5Ai–5Al), or the App-CTF produced by β-secretase cleavage (Figures 5Am–5Ap); (4) immunostaining for App and for

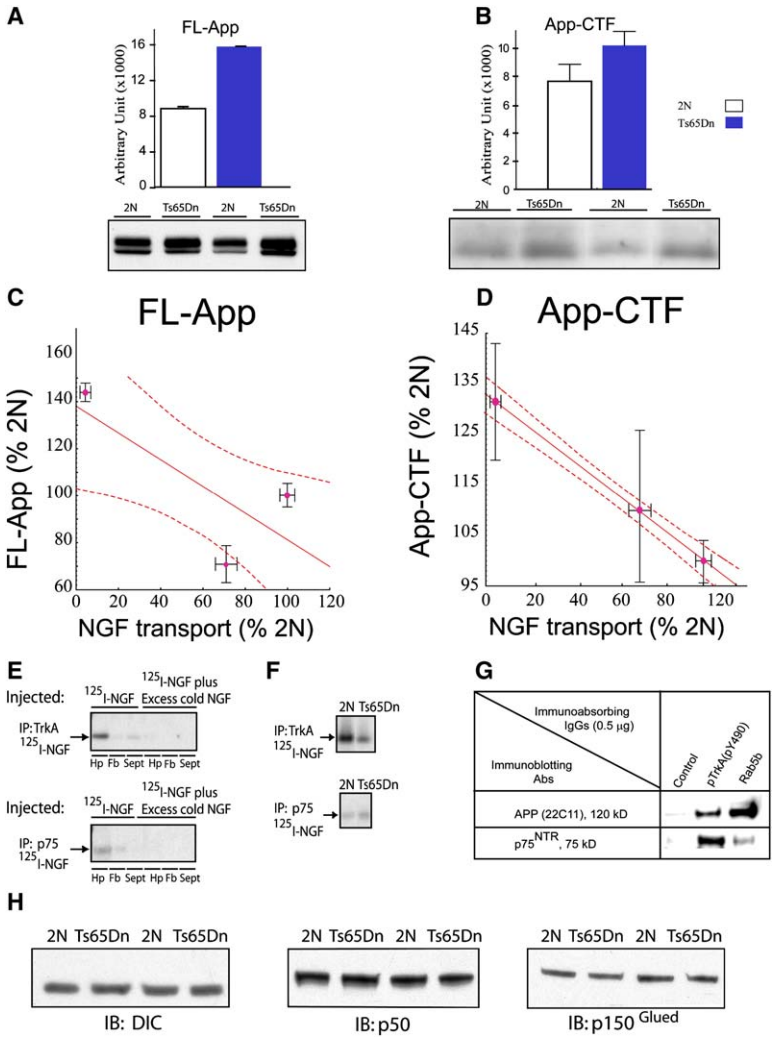

Figure 4. App Metabolism, Function, and Localization in Ts65Dn Mice

(A and B) Western blot depicting the levels of FL-App and App-CTF in synaptosomes prepared from the hippocampus of 2N and Ts65Dn mice (Arbitrary Units; FL-App: 2N = 8868.5 ± 26.16, Ts65Dn = 15873.5 ± 41.72; App-CTF: 2N = 7632.5 ± 1195.71, Ts65Dn = 10162.5 ± 989.24; n = 2, with each experimental group using the tissues of three mice).

(C and D) Correlation between the levels of FL-App or its CTFs (C-83 plus C-99) in hippocampus and NGF transport. FL-App (percent 2N): 2N = 100.0 ± 4.5, n = 4; Ts1Cje, 70.70 ± 8, n = 3; Ts65Dn = 143.8 ± 4.1, n = 4; 2N versus Ts1Cje, p = 0.149, 2N versus Ts65Dn, p = 0.020); App-CTFs: 2N = 100.0 ± 3.3, n = 4; Ts1Cje = 109.89 ± 16.71, n = 3; Ts65Dn = 131.43 ± 11, n = 4; 2N versus Ts1Cje, p = 0.723, 2N versus Ts65Dn, p = 0.021). There was no significant linear correlation between FL-App and NGF transport (r = −0.7582, p = 0.452), but a significant negative correlation was detected between the amount of App-CTFs and NGF transport (r = −0.999, p = 0.007).

(E and F) Immunoprecipitation of radiolabeled NGF following hippocampal injections in vivo. (E) 18 hr following injection of radiolabeled NGF, the hippocampus (Hp), fimbria-fornix (Fb) and septum (Sept) were dissected and homogenized, and lysates were immunoprecipitated first with antibodies to TrkA and then to $p75^{NTR}$. NGF bound to its receptors was detected in immunoprecipitates after SDS-PAGE and blotting by exposing membranes to phosphoimaging. Though, as expected from direct assay of radioactivity, much less NGF was detected in immunoprecipitates of fimbria-fornix and septum, we routinely detected a signal that was above background in 2N mice, indicating that NGF was internalized and transported on its receptors. Specific binding and internalization is evident in the absence of a signal above background in experiments in which a 200-fold excess of NGF was injected together with radiolabeled NGF. (F) NGF was bound to TrkA and to $p75^{NTR}$ in the hippocampus of both 2N and Ts65Dn mice. Because immunoprecipitations did not quantitatively bring down NGF, no attempt was made to compare the amount of NGF recovered from different tissues or between 2N and Ts65Dn mice.

(G) Immunoisolation of EEs from PC12 cells showed that TrkA is present in the same endosomes as App and that App is present together with $p75^{NTR}$ in EEs that contain Rab5b.

(H) Western blotting for the DIC, $p150^{Glued}$, and p50 dynamitin showed no alterations in levels in hippocampal synaptosomes from Ts65Dn mice. Error bars = SEM.

App-CTF is increased in cholinergic terminals of Ts65Dn mice (Figures 6Aa–6Ah and 6Bb and 6Bc) ; and (5) App and App-CTF are present in EEs in cholinergic terminals in both Ts65Dn and 2N mice (Figures 5Am–5At, Figure 6Bd, Table S5). Given extensive colocalization of App and App-CTF with Rab5b in VAChT-positive terminals in both Ts65Dn and 2N mice (~100% for App; for App-CTF, see Table S5), we conclude that the increase in App and App-CTF in cholinergic axons includes EEs.

To determine whether or not NGF was also present in EEs in BFCN axons, we incubated hippocampal slices with biotinylated NGF (Bt-NGF) and stained with streptavidin Quantum dots. NGF was robustly detected in structures whose shape corresponded to axons; the vast majority of NGF (~91%) was present in cholinergic axons, as indicated by colocalization with VAChT (not shown). Staining for NGF was extensively colocalized with that for Rab5b in both Ts65Dn and 2N mice (Figures 5Ba–5Bd). The presence of NGF within EEs was due to specific binding and internalization because staining was eliminated when sections were incubated with Bt-NGF in the presence of a 500-fold excess of unlabeled NGF (not shown). Next we gathered evidence that TrkA and $p75^{NTR}$, the receptors for NGF which are present in BFCNs and their axons (Jaffar et al., 2001; Yeo et al., 1997), mediated NGF binding and internalization. After injecting radiolabeled NGF into the hippocampus in vivo, we could immunoprecipitate NGF bound specifically to both TrkA and $p75^{NTR}$ in the hippocampus; as expected, smaller amounts were immunoprecipitated from the fimbria-fornix and septum (Figure 4E). Moreover, NGF was readily detected in immunoprecipitations for both receptors in the hippocampus of both 2N and Ts65Dn mice (Figure 4F). $p75^{NTR}$ was present within cholinergic axons (Figures 5Be–5Bh). Because of limited availability of antibodies, we were not able to show directly that

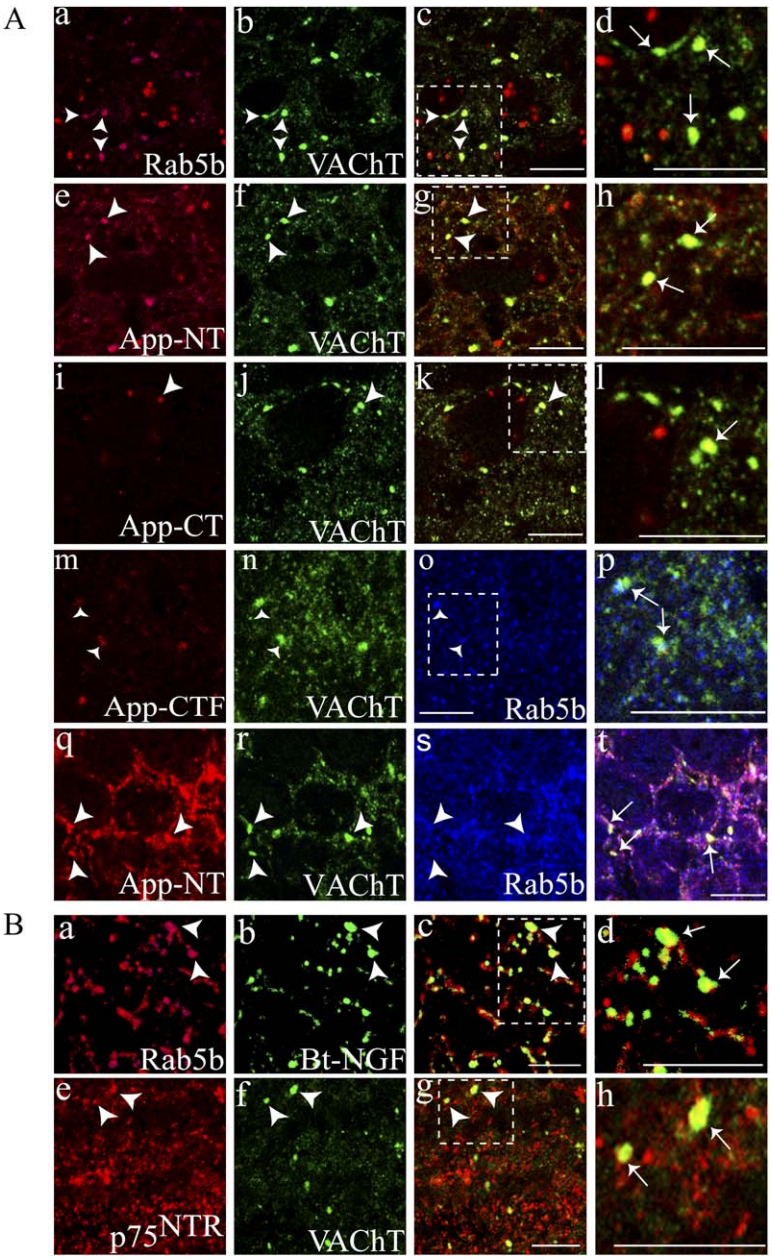

Figure 5. The Presence of App and NGF Receptors in EEs in Cholinergic Terminals

(A) Confocal microscopy studies in the CA2 area of 2N hippocampus examining colocalization of markers for cholinergic axons (VAChT), EEs (Rab5b), App, CTF-App and $p75^{NTR}$. Colocalization was detected for Rab5b and VAChT (Aa–Ad) and VAChT and App in EEs (Rab5b), using antibodies directed against the N terminus (Ae–Ah), C terminus (Ai–Al), or App-CTF (Am–Ap). EEs also were found to contain App in cholinergic terminals (Aq–At). Scale bar, 10 μm (Aa–Ap), 5 μm (Aq–At).

(B) Bt-NGF, specifically bound and internalized in hippocampal slices, was extensively colocalized in Rab5b-Ir structures (Ba–Bd). $p75^{NTR}$-Ir was present in cholinergic axon terminals (Be–Bh). Scale bar, 10 μm (Ba–Bh).

The same patterns for colocalization were evident in the Ts65Dn hippocampus (not shown). Dotted areas are enlarged in the adjacent panels to the right. Arrows show colocalization. The OD of Rab5b positive puncta within BFCN terminals was less in Ts65Dn mice (2N = 144 ± 1.4 OD, Ts65Dn = 135 ± 1.72 OD, p = 0.001).

$p75^{NTR}$ and TrkA were present in EEs in BFCN axons. However, there is strong evidence that both receptors are present in EEs in other NGF-responsive cells (Delcroix et al., 2003). Finally, we could demonstrate that NGF and its receptors are present together with App in EEs. In a fraction enriched in EEs from PC12 cells, we showed in immunoadsorption studies that membranes adsorbed with antibodies for either Rab5b or for pTrkA also contained App and $p75^{NTR}$ (Figure 4G). We conclude that increased App expression is registered in EEs of BFCN axons and that these endosomes also contain NGF that is specifically bound and internalized via its receptors.

NGF-Containing EEs Are Abnormal in Ts65Dn Mice

To explore further the status of EEs in cholinergic terminals, we examined their size and immunostaining properties in the hippocampus of Ts65Dn and 2N mice. There was no change in the average size of EEs in Ts65Dn (2N = 0.34 ± 0.02 μm^2; Ts65Dn = 0.31 ± 0.03 μm^2, p = 0.32), but we did note a small but significant change in the intensity of Rab5b immunostaining in the Ts65Dn hippocampus (OD: 2N = 144 ± 1.4; Ts65Dn = 135 ± 1.72, p = 0.001). To examine specifically the EEs that contain App, we carried out triple-labeling studies. The findings were as follows: (1) both App and App-CTF were extensively localized in EEs in cholinergic terminals (Table S5), and (2) there was significant enlargement of these EEs (for App N terminus see Figure 6Bd; App-CTF: 2N = 0.260 ± 0.016 μm^2, n = 3; Ts65Dn = 0.407 ± 0.03, n = 3, p = 0.002). To examine the EEs that contain NGF, hippocampal slices were incubated with Bt-NGF and then processed for immunostaining for Bt-NGF and Rab5b. In the Ts65Dn hippocampus, we

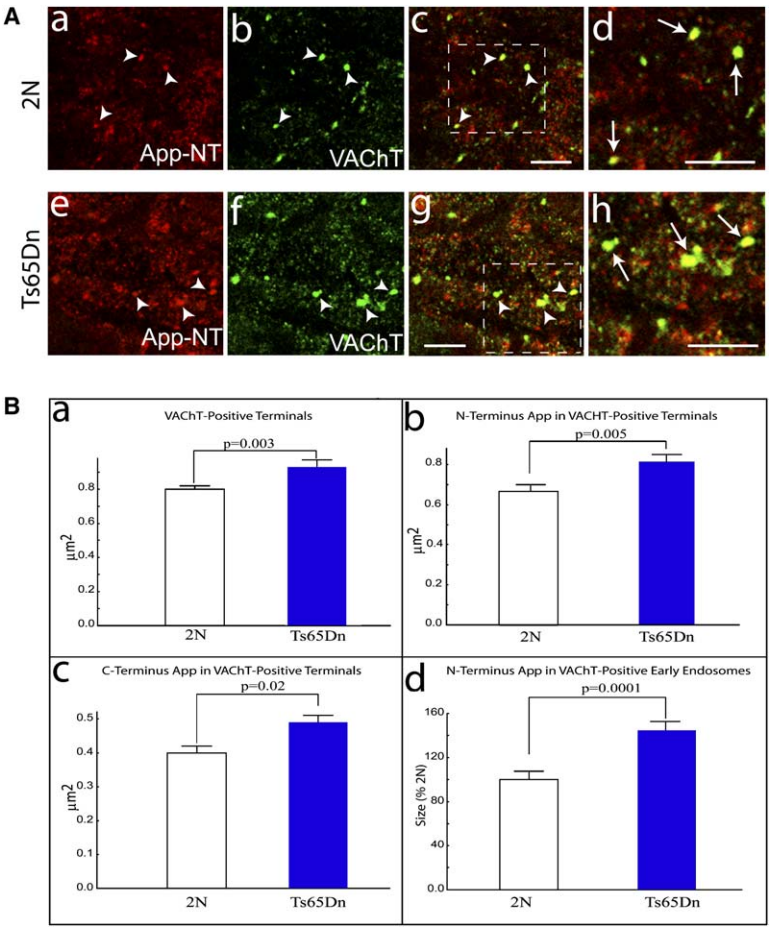

Figure 6. App in EEs in Cholinergic Terminals in Ts65Dn and 2N Mice

(A) Photomicrographs depicting App N terminus in VAChT-positive terminals in the CA2 area of the hippocampus of 2N (Aa–Ad) and Ts65Dn (Ae–Ah) mice. App-positive cholinergic terminals were found to be enlarged in Ts65Dn mice. Dotted areas are enlarged in the adjacent panels to the right. Arrows show colocalization. Scale bar, 10 μm (Aa–Ah).

(B) Quantitative analysis indicated that the size of VAChT-positive terminals was significantly increased in Ts65Dn mice (2N = 0.80 ± 0.02 μm^2, Ts65Dn = 0.93 ± 0.04 μm^2, p = 0.003 [Ba]). In addition, the amount of App immunostaining of both N terminus (Bb) and C terminus (Bc) in VAChT-positive terminals was significantly increased in Ts65Dn mice (N terminus: 2N = 0.69 ± 0.03 μm^2, Ts65Dn = 0.83 ± 0.04 μm^2, p = 0.005; C terminus: 2N = 0.40 ± 0.02 μm^2, Ts65Dn = 0.49 ± 0.03 μm^2, p = 0.02). The size of App N terminus-positive-EEs (Bd) in cholinergic terminals was significantly larger in Ts65Dn compared with 2N mice (2N = 100% ± 7.2%, n = 6; Ts65Dn = 144.67% ± 7.9%, n = 5; p = 0.0001).

Error bars = SEM.

detected a significant increase in the area of colocalization for NGF and Rab5b, pointing to an increase in the size of EEs that contain NGF. Indeed, the average size was increased to ~180% of that in 2N mice (2N = 0.69 ± 0.06 μm^2, n = 4; Ts65Dn = 1.24 ± 0.12 μm^2, n = 3; p < 0.001). Taken together, the data are evidence for the presence in cholinergic terminals of Ts65Dn mice of enlarged EEs that contain NGF, App, and App-CTF. Whether or not the defect in NGF transport is linked to a change in endosomal size or function, and the relationship (if any) to overexpression of *App*, is yet to be established.

Evidence for Selective Disruption of Retrograde Transport in Ts65Dn Mice

In view of prior studies showing that both TrkA and $p75^{NTR}$ are engaged in retrograde transport of NGF (Kiss et al., 1993), the marked decrease in transport detected herein suggests that both receptors are affected. Remarkably, however, the defect in transport is not general because we detected no decrease in the retrograde transport of Fluoro-Gold (FG); (percent area covered by FG fluorescence [mean ± SEM] [n = 7]: 2N = 8.85% ± 1.9%; Ts65Dn = 8.85% ± 1.24%; p = 0.949; Figures 7A and 7B), a molecule widely used to examine retrograde transport (Wessendorf, 1991). Because cholinergic neurons represent the principle source of afferents to the hippocampus from MSN, the data are evidence against a universal, marked defect in retrograde transport in these neurons. In concert with this finding, we also failed to detect changes in components of the dynein-dynactin complex in the Ts65Dn hippocampus (Figure 4H). Thus, disrupted retrograde transport may affect a subset of endosomal cargoes.

Discussion

Our studies establish a link between disrupted retrograde transport of NGF, a target-derived neurotrophic factor for BFCNs, and the degeneration of these neurons in Ts65Dn mice, which are segmentally trisomic for mouse chromosome 16 and serve as a model for DS. We used a genetic approach to show that increased gene dose for *App* contributes to the creation of both phenotypes. Deleting a copy of *App* in trisomic mice led to a marked improvement in NGF transport and BFCN morphology. NGF transport was compromised significantly, but to a lesser extent, by transgenesis for either wt or mutant *APP*, thus confirming that increased expression of this gene is linked to the transport defect. However, in these mice there was no evident degeneration of BFCNs. Taken together, the findings are evidence that in the context of trisomy for mouse genes homologous to those on human chromosome 21, increased gene dose and overexpression of App compromises NGF transport and promotes degeneration of BFCNs.

The retrograde transport of target-derived neurotrophic factor signals plays an important role in the survival,

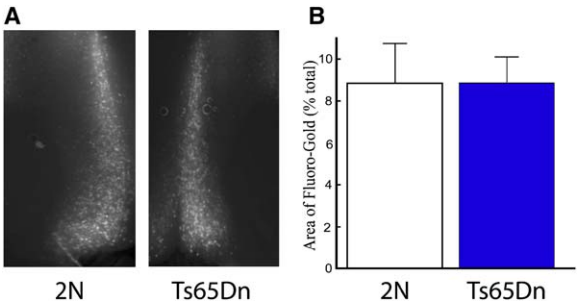

Figure 7. Retrograde Transport of Fluoro-Gold in Ts65Dn Mice

(A) Fluoro-Gold transport to the MSN in 2N and Ts65Dn mice, visualized with UV illumination.

(B) There was no significant difference between the total area covered by FG between 2N and Ts65Dn mice (2N = 8.85 ± 1.9, n = 7; Ts65Dn = 8.85 ± 1.25, n = 7). Note that there also was no difference between genotypes in the area identified as MSN.

Error bars = SEM.

differentiation, and maintenance of many neurons. An increasing body of evidence supports the view that retrograde transport of signaling endosomes, in which the neurotrophic factor remains bound to its receptor, is an important means by which trophic signals are moved (Howe and Mobley, 2004; Zweifel et al., 2005). The close correlations between the NGF transport and BFCN degenerative phenotypes demonstrated herein in models of DS are evidence to support the view that disrupted NGF transport is responsible for BFCN degeneration. A causal role is supported by studies showing a correlation between NGF levels in targets of innervation of mature neurons and the status of key parameters, including the expression of neurotransmitter genes and the size of cell bodies (Sofroniew et al., 1993). Indeed, experiments in which NGF levels are reduced through gene disruption or production of neutralizing antibodies create phenotypes quite similar to those seen in the Ts65Dn mouse (Capsoni et al., 2000; Chen et al., 1997). Moreover, decreased NGF transport to the cell bodies of BFCNs in the aged rat was correlated with atrophy (Cooper et al., 1994). Finally, as noted above, when delivered by a method that obviated the need for retrograde transport, NGF treatment rescued BFCN phenotypes in Ts65Dn mice. The current findings thus provide compelling support for the view that failed NGF transport is responsible for BFCN degeneration in the Ts65Dn mouse. Nevertheless, to demonstrate that NGF transport failure in Ts65Dn mice causes degeneration of BFCNs will require studies in which specifically disrupting NGF signaling is shown to prevent the rescue of the degenerative phenotype achieved by reducing *App* gene dose in these mice.

One may question whether failed NGF retrograde transport is specific to this neurotrophin (NT). BDNF and NT3 are also transported in BFCNs and conceivably could be affected. In an attempt to address this point, in an earlier study (Cooper et al., 2001) we examined transport of the NTs BDNF and NT3 using the same methods as for the current study; we found that transport was below the limits of detection. Thus, it would appear that transport of these NTs is less robust than for NGF. To address the issue of specificity in the current study, we carried out studies using FG, a marker often used to examine retrograde transport. Our FG injection study showed no differences between Ts65Dn and 2N mice, pointing to no generalized failure in retrograde transport in these mice. The result encourages the view that many cargoes may be moved normally, but does not rule out defect in the transport of other NT cargoes. Indeed, we expect that such defects may exist. Transport studies examining a variety of cargoes will be needed to fully define the defect.

It is of interest to consider the time course for the defects in NGF transport in relation to changes in BFCNs. Based on our current findings and those provided previously (Cooper et al., 2001), decreased NGF transport precedes neuropathological changes in BFCN cell bodies in Ts65Dn mice by at least 9 months. Indeed, the defect was present at the earliest age examined, 3 months (not shown). At 3 months, there is also evidence of abnormal EEs, as documented herein. Moreover, there are changes in the distribution of BFCN axons as early as 6 months. Thus changes in both axonal structure and function predate changes in the size and number of cell bodies of BFCNs. Whether or not axonal changes predate more subtle pathological alterations in BFCN somas will require additional ultrastructural studies.

Given the correlations demonstrated between *App* gene dose and protein levels in the DS models, our results are evidence that, in the context of the other genes present in Ts65Dn mice, increased levels of App and/or its products contribute conspicuously to marked decreases in NGF transport and to the pathogenesis of degeneration. It is an open question as to whether or not increased expression of *App* alone is sufficient to cause BFCN dysfunction. Though we detected significant decreases in NGF transport, Tg human *APP* was not associated with obvious degenerative changes. It is perhaps noteworthy that the defect in NGF transport in *APP* Tg mice (40% to 60% of non-Tg) was approximately the same as in Ts65Dn mice deleted for one copy of *App* (~50%) and far less severe than in Ts65Dn mice (~10%). Moreover, while we detected no change in the distribution of BFCN axons within hippocampus of APP_{Swe} mice, a recent study did demonstrate the presence of large varicosities in these axons well before the deposition of plaques (Stokin et al., 2005), showing that more subtle degenerative phenotypes are present. Conceivably, such changes could be linked to impaired NGF transport.

In pointing to the importance of gene dose and overexpression of a specific gene in the setting of trisomy, the current study is expected to enhance progress in understanding the cellular mechanism of pathogenesis for neurodegeneration in DS. It makes the argument that even in the context of a complex genetic lesion, increased dose for but one gene can impact important features of neuronal structure and function. Though other genes in the trisomic segment must contribute to the defect in NGF transport and to degenerative changes, our report draws attention to a surprisingly robust effect of the dose for *App*. It is noteworthy that a patient with partial trisomy for human chromosome 21 that did not include the *APP* gene exhibited no age-related cognitive decline and no AD-related pathology (Prasher et al., 1998). It is intriguing then that increased gene dose for *APP* may contribute significantly to the pathogenesis

of AD-related changes and dementia in people with DS, including the degeneration of BFCNs. If so, treatments to reduce *APP* gene expression may prove valuable. In documenting the importance of gene dose, the current findings also recall the neurodegenerative phenotypes created by small changes in the doses of other wild-type genes in Charcot-Marie-Tooth disease Type 1A (Lupski et al., 1991), Pelizaeus Merzbacher disease (Hodes et al., 2000), Parkinsonism (Singleton et al., 2003), and Rett syndrome (Van Esch et al., 2005). Indeed, a recent report links an increase in gene dose for *APP* in several families with early onset AD with cerebral amyloid angiopathy (Rovelet-Lecrux et al., 2006). While the degenerative mechanism induced by increased gene dose and expression will almost certainly be specific to the disorder in question, it is apparent that for some genes even apparently small departures from normal can seriously perturb neuronal function and viability.

Our findings motivate studies to examine what role is played by App in endosomal transport, and what changes are induced by increased *App* gene expression in the trafficking of neurotrophic signals. The first step is to elucidate which products of App contribute and where they act. Given the early appearance of Aβ-containing plaques in the brains of individuals with DS (Lemere et al., 1996), and the demonstration that the Aβ peptide is responsible for cellular toxicity both in vivo and in vitro (see Bossy-Wetzel et al., 2004 and Selkoe, 2002) we considered whether or not Aβ compromises NGF transport in the Ts65Dn mouse. Remarkably, we detected no increase in the levels of Aβ peptides in the Ts65Dn mouse. We conclude, therefore, that this peptide is unlikely to contribute to the NGF transport failure in these mice. In Ts65Dn mice, a much more convincing case can be made for increased levels of FL-App and the App-CTFs. Indeed, the levels of App-CTFs were significantly inversely correlated with NGF transport, raising the possibility that this species may play a role. Unanswered is the question as to whether or not increased levels of Aβ would impair NGF transport in other Tg mice, including those that model the neuropathology of AD. Human Aβ40 and Aβ42 are readily measurable in mice Tg for either APP_{Swe} or for both APP_{Swe} and $PS1_{A246E}$ (Borchelt et al., 1996; G. Stokin, unpublished data) and elderly mice of each genotype show evidence of AD-related pathology (Borchelt et al., 1997). Therefore, a role for increased Aβ peptide in contributing to the NGF transport defect in these mice cannot be excluded.

Pointing to an intra-axonal locus for disrupting transport, earlier studies showed that NGF binding and internalization in hippocampal synaptosomes was not decreased (Cooper et al., 2001), findings recapitulated herein in Tg *APP* mice. Remarkably, in mice Tg for only mutant *PS1*, we detected increases in NGF binding, internalization, and transport. Given that these measures were normal in the doubly Tg mice ($APP_{Swe}/PS1_{A246E}$), the results were surprising. While a number of possibilities can be offered to explain the findings, we note that others have shown that expressing mutant *PS1* restricts APP trafficking in axons (Cai et al., 2003). As a speculation, preventing entry of APP into axons may enhance anterograde trafficking of NGF receptors to axon terminals, a change that would be most evident in the absence of increased *APP* expression. The increase in retrograde transport would then simply reflect an increase in binding and internalization of NGF. Alternatively, in addition to enhancing anterograde transport, mutant PS1 may to a lesser extent also reduce retrograde transport of NGF. This would result in a mismatch between binding and internalization on the one hand and transport on the other. Indeed, we noted that the increase in transport in mutant PS1 mice (~40%) was not as large as that for internalization (~100%). Under this view, mutant PS1 acting alone would both increase delivery of NGF receptors to axon terminals and also modestly compromise NGF retrograde transport. An effect of mutant PS1 on retrograde transport would then further exacerbate the decrease in transport in mice transgenic for both APP_{Swe} and $PS1_{A246E}$. While noting that the magnitude of the increased deficit in transport between APP_{Swe} and the doubly transgenic mice might well be explained in this way, we believe that other interactions between the products of these transgenes may also contribute.

Finally, the current study raises the possibility that the EE constitutes a potential locus for disrupted NGF transport within cholinergic axons in Ts65Dn mice. Immunostaining for App and App-CTF is increased in EEs and this same compartment contains NGF and its receptors. Moreover, we provide evidence that these EEs contain NGF and are enlarged in the Ts65Dn hippocampus, showing that this compartment is abnormal. In view of earlier studies linking enlargement of EEs and *App* gene dose in the Ts65Dn mouse (Cataldo et al., 2003), and the important role played by EEs in retrograde transport of NGF and its signals (Delcroix et al., 2004), it is tempting to speculate that increased App in EEs is implicated in the NGF transport defect. However, this association is far from certain. Indeed, Cataldo and coworkers failed to see the increase in EE size in mice Tg for APP, while in the current study we show decreased transport of NGF in such mice. One possibility is that an endosomal abnormality other than size is linked to increased presence of App and abnormal transport. But important alternatives to abnormal endosomes can be envisioned to play a role, including, for example, changes in the axonal cytoskeleton and the provision of ATP for retrograde motors. Future studies will be needed to define the mechanism and locus for failed transport and neurodegeneration in Ts65Dn mice.

Our findings build on an emerging story for the importance of failed axonal transport in neurodegeneration (Goldstein, 2003; Salehi et al., 2003). In so doing, they suggest that a focus on this aspect of the biology of DS may provide insights into DS, AD and other disorders with age-related neurodegeneration.

Experimental Procedures

Mice

Ts65Dn and Ts1Cje Mice

Age-matched controls were used for all experiments. Unless otherwise noted, only males were used. The Ts65Dn mouse colony was maintained by crossing Ts65Dn females (originally obtained from Jackson Laboratory, Bar Harbor, ME) to C57BL/6JEi × C3H/HeSnJ (B6EiC3Sn) F1 males (Jackson Laboratory). Fibroblasts or lymphocytes were karyotyped to identify 2N and Ts65Dn mice. To generate Ts1Cje mice on a similar genetic background, Ts1Cje mice on the

C57BL/6JEi background were crossed with C3H/HeSnJ mice and the resulting Ts1Cje mice were crossed to B6EiC3Sn F1 mice (Sago et al., 1998). Ts1Cje mice were genotyped using multiplex polymerase chain reaction (PCR) primers for neomycin (*Neo*) and for a glutamate receptor, ionotropic, Kainite 1 (*Grik1,* as internal control) as previously described (Sago et al., 1998). All mouse breeding was approved by the Committee on Animal Research at the centers involved (Stanford University, UCSF, UCSD, and Case Western Reserve University) and all the studies using mice were approved by the Stanford University Committee on Animal Research.

Ts65Dn Mice Carrying Only Two Copies of Amyloid Precursor Protein

In order to generate Ts65Dn:$App^{+/+/-}$ mice, Ts65Dn female mice were mated with male mice hemizygous for *App*, in which *App* was inactivated by deleting the *App* promoter and its first exon (Zheng et al., 1996). Male hemizygous *App* mice were kept on the C57BL/6J background. The product of litters included 2N mice with two copies of *App* (2N:$App^{+/+}$), 2N mice with one copy of *App* (2N:$App^{+/-}$), Ts65Dn mice with the three copies of *App* (Ts65Dn:$App^{+/+/+}$), and Ts65Dn mice with two copies of *App* (Ts65Dn:$App^{+/+/-}$).

Wild-Type APP Transgenic Mice

Mice harboring a YAC of 650 kb containing the gene for human *APP* were produced as indicated (Lamb et al., 1993) and carried on the C57BL/6J background.

APP_{Swe}, *Presenilin 1* (PS1)$_{A246E}$, APP_{Swe}/PS1$_{A246E}$, *and Their Non-Tg Littermates*

These mice were maintained on a mixed (C3H/HeJ and C57BL/6J) background. The APP_{Swe} mouse expresses a chimeric mouse/human *APP*695 containing the human Aβ domain and mutations (K595N, M596L) linked to FAD (Goate et al., 1991). $PS1_{A246E}$ mice carry a mutant transgene for human *PS1* (A246E) (Borchelt et al., 1997). To generate doubly Tg mice (i.e., APP_{Swe}/$PS1_{A246E}$ mice), APP_{Swe} mice (C3H/HeJ × C57BL/6J) were crossed with $PS1_{A246E}$ (C3H/HeJ × C57BL/6 F3) mice.

Retrograde Transport Studies

NGF

NGF was iodinated and injected stereotactically in hippocampus as described (Cooper et al., 2001, see also Supplemental Experimental Procedures). 2N, Ts1Cje, and Ts65Dn used for transport studies were 6 to 7 months old. *APP* wt-Tg, non-Tg, Ts65Dn:$App^{+/+/+}$, and Ts65Dn:$App^{+/+/-}$ mice were 10 to 12 months old. APP_{Swe}, $PS1_{A246E}$, APP_{Swe}/$PS1_{A246E}$, and the non-Tg control mice were 19–20 months old.

Fluoro-Gold

Twelve-month-old 2N and Ts65Dn mice were anesthetized with a combination of ketamine (60 mg/kg, i.p.) and xylazine (12 mg/kg), both injected i.p. and placed in a stereotaxic apparatus. Using a mouse brain atlas (Hof et al., 2000), unilateral injections (0.2 μl each over 12 min) were made with Fluoro-Gold (Fluorochrome, Inc, Englewood, CO; 4% in water) at three sites encompassing the rostrocaudal extent of the hippocampus. After 24 hr, mice were deeply anesthetized, perfused, and postfixed in 4% paraformaldehyde overnight at 4ºC prior to dehydration in 20% sucrose overnight and vibratome sectioning (200 μm). Sections were mounted and coverslipped. Retrograde labeling was analyzed under epifluorescence illumination with a Nikon microscope coupled to a Spot Camera (Diagnostic Instruments Inc, MI). Images were captured and then thresholded to yield a distribution for pixels that conformed to the intensity of staining as determined visually. The area for analysis was the MSN, as masked to account for the distribution of labeled cells. The percentage of this area covered by label was then determined (Image Pro Plus).

Cholinergic Neuron Morphology

BFCN Cell Bodies in the MSN

BFCNs were identified by immunohistochemical staining for $p75^{NTR}$, an NT receptor that is localized specifically to cholinergic neurons in the basal forebrain (Koh and Loy, 1989); in other experiments these neurons were detected using immunostaining for TrkA (Holtzman et al., 1995, see also Supplemental Experimental Procedures). Nineteen- to twenty-two-month-old 2N, Ts1Cje, and Ts65Dn mice were used for these morphological studies.

BFCN Innervation of Hippocampus

To examine cholinergic axons in the hippocampus, we examined the overall intensity of immunostaining for $p75^{NTR}$ and ChAT in the hippocampus (see Supplemental Experimental Procedures).

Immunostaining Studies

Colocalization Studies for $p75^{NTR}$ and ChAT in Neurons of the Medial Septum

2N and Ts65Dn mice were perfused, and sections were stained and analyzed for colocalization between $p75^{NTR}$ and ChAT as described in the Supplemental Experimental Procedures. One 2N and one Ts65Dn (both 3.5 months of age) were used for these studies.

Examining Rab5b, APP, and $p75^{NTR}$ in Cholinergic Axons in the Hippocampus

Immunostaining studies were used to define the presence of Rab5b, App, and $p75^{NTR}$ in cholinergic terminals visualized by using an antibody against VAChT (AB1578, Chemicon; 1:500), the transporter for acetylcholine (Cobb et al., 1999). Hippocampal sections were prepared, stained, and analyzed using confocal microscopy as described in the Supplemental Experimental Procedures. 2N and Ts65Dn mice (age 3 to 4 months) were used for all these studies.

Defining the Locus of NGF that Is Bound and Internalized Using Bt-NGF in Hippocampal Slices

We used Bt-NGF to define the locus of NGF that is bound and internalized in hippocampus. NGF was biotinylated using EZ-link biotin-PEO-amine (Pierce, Rockford, IL) according to a published protocol (Bronfman et al., 2003). Bt-NGF was fully active biologically, as examined by its potency in induction of TrkA phosphorylation (pTyr 490) in PC12 cells. Hippocampal slices were prepared for Bt-NGF binding and internalization studies as described (Kleschevnikov et al., 2004, see also Supplemental Experimental Procedures). Three- to four-month-old Ts65Dn (n = 2) and 2N (n = 2) mice were used for these studies.

Immunoprecipitation of Radiolabeled NGF following Injection In Vivo

^{125}I NGF (0.3 μl) was injected in the hippocampus as described above. At 12 hr after injection, brains were removed and the hippocampus, fimbria-fornix, and septum were rapidly dissected and studied as described in the Supplemental Experimental Procedures. Three-month-old 2N and Ts65Dn mice were used for these studies.

Immunoisolation of EEs

An EE-enriched fraction was isolated from NGF-treated PC12 cells using an established method (Wu et al., 2001). The membrane fraction was collected. An aliquot (50 μg total protein) was reconstituted to 1 ml PBS2+ (PBS with 0.9 mM CaCl2, 0.5 mM MgCl2) containing 1% BSA, 0.1 mM PMSF, 1 mM Na3VO4. Samples were incubated with 0.5 μg IgGs and 30 μl of mMACS Protein A or G MicroBeads (Miltenyi Biotec) on ice for 1 hr. The samples were then loaded onto MACS Separation columns, washed, and eluted. The eluents were analyzed by sodium dodecyl sulfate-polyacrylamide gel electrophoresis (SDS-PAGE) and immunoblotting. These experiments were repeated at least three times with the same result.

NGF Binding and Internalization in Synaptosomes

These studies were conducted essentially as described (Cooper et al., 2001, see also Supplemental Experimental Procedures). The data report the results of the following number of mice (non-Tg = 4, APP_{Swe} = 4, APP_{Swe}/$PS1_{A246E}$ = 4, $PS1_{A246E}$ = 4) at age 18 to 24 months.

App and *NGF* mRNA Measurements

Eighteen-month-old 2N, Ts1Cje, and Ts65Dn mice were deeply anesthetized with sodium pentobarbital (200 mg/kg i.p.), transcardially perfused with ice-cold normal saline and studied for *App* and *NGF* gene expression (see Supplemental Experimental Procedures).

Western Blot Studies

App

Ts65Dn and Ts1Cje Mice and Their 2N Controls. Ts65Dn and 2N mice were euthanized with sodium pentobarbital (200 mg/kg i.p.)

(Abbott Laboratories, North Chicago, IL). The brains were quickly removed and several brain regions, including hippocampus, were dissected on ice prior to storage at −80ºC. Brain samples were homogenized in HEPES-buffered saline (50 mM HEPES [pH 7.4], 0.15 M NaCl, and 5 mM EDTA containing a protease inhibitor cocktail; Sigma Chemical Company) and centrifuged at 2500 × g for 10 min and supernatants were collected for further analysis. Western blots were used to determine the levels of FL-App and its App-CTF (C-83 plus C-99) after loading 2, 3, and 4.5 μg of the extract onto SDS-PAGE gels (BioRad Criterion 10%–20%) (Sambamurti et al., 1992). APP was detected using a rabbit antibody to the C-terminal 20 residues APP (O443) as described previously (Pinnix et al., 2001). Images from multiple repeats of each sample were run on independent gels and scanned images were quantified using ImageQuant software (Amersham Corporation, Piscataway, NJ). To avoid the variation due to differences in exposure of films, we normalized the values for each gel using the average of all quantified bands. Eleven-to twelve-month-old 2N, Ts1Cje, and Ts65Dn mice were used in the App protein studies.

Ts65Dn:$App^{+/+/-}$ *and Ts65Dn:*$App^{+/+/+}$ *Mice and Their 2N Controls.* The cerebral cortex was homogenized in 0.2% diethylamine (DEA/50 mM NaCl) and processed as described (Petanceska et al., 2000). Samples were solubilized in 2% SDS/PBS containing 7 μg/ml aprotinin, 1 μg/ml leupeptin, and 1 mM phenylmethylsulphonylfluoride, then sonicated and boiled. The protein concentrations were determined using a bicinchoninic acid (BCA) protein assay kit (Pierce, Rockford, IL). Twenty-five micrograms total proteins were loaded per lane onto 4%–20% Tris-Glycine gels (Invitrogen, Carlsbad, CA) and separated by electrophoresis at 100 volts for 1 hr. APP was detected by Western blotting using a polyclonal antibody CT695 (Zymed, South San Francisco, CA) directed against the C terminus of human APP. Immunoblots were scanned using an Agfa Duoscan *f*40 scanner (Germany) and analyzed by the NIH Image (Bethesda, MD). Mice at 16 months of age were used for this study.

Adaptor Proteins

Synaptosomes from the hippocampi of Ts65Dn and 2N mice were prepared as described above. The protein levels for dynein intermediate chain (DIC) (Santa Cruz Biotechnology), $p150^{Glued}$, and p50 (both from BD, Franklin Lakes, NJ), were examined using SDS/PAGE and Western blotting. Six-month-old mice (2N and Ts65Dn) were used; each experimental group, of which there were two, was comprised of three mice (2N, n = 3; Ts65Dn, n = 3).

Aβ ELISA Measurements

Eighteen-month-old 2N and Ts65Dn mice were euthanized and brains were removed and dissected on ice prior to freezing in liquid nitrogen. Brain samples were studied for Aβ40 and Aβ42 levels as described in the Supplemental Experimental Procedures.

NGF ELISA Measurements

Ts1Cje and 2N mice were euthanized with CO_2 and their brains were removed. The hippocampus was dissected and immediately frozen on dry ice and stored at −80ºC. Samples were homogenized and analyzed for NGF protein using an ELISA from Chemicon, as described, using mouse NGF as the standard (Cooper et al., 2001). Twenty-month-old 2N and Ts1Cje mice were used for this study.

Statistics

Statistica 6 (Tulsa, OK) was used for all analyses, except for NGF transport studies, for which Microsoft Excel was used. Student's t test was used for all transport studies. Data on BFCN cell size and number and NGF transport were analyzed using Kruskal Wallis ANOVA and Mann-Whitney U tests. A value of $p < 0.05$ was considered statistically significant.

Supplemental Data

The Supplemental Data for this article can be found online at http://www.neuron.org/cgi/content/full/51/1/29/DC1/.

Acknowledgments

This research was sponsored by grants from the NIA (AG16999, W.C.M.), NINDS (NS38869, W.C.M.), NICHD (31498, C.J.E.), Adler Foundation (J.D.D.), Alzheimer Association and State of California Alzheimer's Program (A.S. and W.C.M.), McGowan Charitable Trust, Larry L. Hillblom Foundation, and the Down Syndrome Research and Treatment Foundation (W.C.M.).

Received: December 2, 2005
Revised: April 14, 2006
Accepted: May 19, 2006
Published: July 5, 2006

References

Auld, D.S., Kornecook, T.J., Bastianetto, S., and Quirion, R. (2002). Alzheimer's disease and the basal forebrain cholinergic system: relations to beta-amyloid peptides, cognition, and treatment strategies. Prog. Neurobiol. *68*, 209–245.

Belichenko, P.V., Masliah, E., Kleschevnikov, A.M., Villar, A.J., Epstein, C.J., Salehi, A., and Mobley, W.C. (2004). Synaptic structural abnormalities in the Ts65Dn mouse model of Down syndrome. J. Comp. Neurol. *480*, 281–298.

Borchelt, D.R., Thinakaran, G., Eckman, C.B., Lee, M.K., Davenport, F., Ratovitsky, T., Prada, C.M., Kim, G., Seekins, S., Yager, D., et al. (1996). Familial Alzheimer's disease-linked presenilin 1 variants elevate Abeta1–42/1–40 ratio in vitro and in vivo. Neuron *17*, 1005–1013.

Borchelt, D.R., Ratovitski, T., van Lare, J., Lee, M.K., Gonzales, V., Jenkins, N.A., Copeland, N.G., Price, D.L., and Sisodia, S.S. (1997). Accelerated amyloid deposition in the brains of transgenic mice coexpressing mutant presenilin 1 and amyloid precursor proteins. Neuron *19*, 939–945.

Bossy-Wetzel, E., Schwarzenbacher, R., and Lipton, S.A. (2004). Molecular pathways to neurodegeneration. Nat. Med. Suppl. *10*, 2–9.

Bronfman, F.C., Tcherpakov, M., Jovin, T.M., and Fainzilber, M. (2003). Ligand-induced internalization of the p75 neurotrophin receptor: a slow route to the signaling endosome. J. Neurosci. *23*, 3209–3220.

Cai, D., Leem, J.Y., Greenfield, J.P., Wang, P., Kim, B.S., Wang, R., Lopes, K.O., Kim, S.H., Zheng, H., Greengard, P., et al. (2003). Presenilin-1 regulates intracellular trafficking and cell surface delivery of beta-amyloid precursor protein. J. Biol. Chem. *278*, 3446–3454.

Capsoni, S., Ugolini, G., Comparini, A., Ruberti, F., Berardi, N., and Cattaneo, A. (2000). Alzheimer-like neurodegeneration in aged antinerve growth factor transgenic mice. Proc. Natl. Acad. Sci. USA *97*, 6826–6831.

Carter, R.E., and Sorkin, A. (1998). Endocytosis of functional epidermal growth factor receptor-green fluorescent protein chimera. J. Biol. Chem. *273*, 35000–35007.

Cataldo, A.M., Petanceska, S., Peterhoff, C.M., Terio, N.B., Epstein, C.J., Villar, A., Carlson, E.J., Staufenbiel, M., and Nixon, R.A. (2003). App gene dosage modulates endosomal abnormalities of Alzheimer's disease in a segmental trisomy 16 mouse model of down syndrome. J. Neurosci. *23*, 6788–6792.

Chen, K.S., Nishimura, M.C., Armanini, M.P., Crowley, C., Spencer, S.D., and Phillips, H.S. (1997). Disruption of a single allele of the nerve growth factor gene results in atrophy of basal forebrain cholinergic neurons and memory deficits. J. Neurosci. *17*, 7288–7296.

Cobb, S.R., Bulters, D.O., Suchak, S., Riedel, G., Morris, R.G., and Davies, C.H. (1999). Activation of nicotinic acetylcholine receptors patterns network activity in the rodent hippocampus. J. Physiol. *518*, 131–140.

Cooper, J.D., Lindholm, D., and Sofroniew, M.V. (1994). Reduced transport of [125I]nerve growth factor by cholinergic neurons and down-regulated TrkA expression in the medial septum of aged rats. Neuroscience *62*, 625–629.

Cooper, J.D., Salehi, A., Delcroix, J.D., Howe, C.L., Belichenko, P.V., Chua-Couzens, J., Kilbridge, J.F., Carlson, E.J., Epstein, C.J., and Mobley, W.C. (2001). Failed retrograde transport of NGF in a mouse model of Down's syndrome: reversal of cholinergic neurodegenerative phenotypes following NGF infusion. Proc. Natl. Acad. Sci. USA *98*, 10439–10444.

Cummings, J.L. (2004). Alzheimer's disease. N. Engl. J. Med. *351*, 56–67.

Davisson, M.T., Schmidt, C., and Akeson, E.C. (1990). Segmental trisomy of murine chromosome 16: a new model system for studying Down syndrome. Prog. Clin. Biol. Res. *360*, 263–280.

Delcroix, J.D., Valletta, J.S., Wu, C., Hunt, S.J., Kowal, A.S., and Mobley, W.C. (2003). NGF signaling in sensory neurons: evidence that early endosomes carry NGF retrograde signals. Neuron *39*, 69–84.

Delcroix, J.D., Valletta, J., Wu, C., Howe, C.L., Lai, C.F., Cooper, J.D., Belichenko, P.V., Salehi, A., and Mobley, W.C. (2004). Trafficking the NGF signal: implications for normal and degenerating neurons. Prog. Brain Res. *146*, 3–23.

Gage, F.H., Batchelor, P., Chen, K.S., Chin, D., Higgins, G.A., Koh, S., Deputy, S., Rosenberg, M.B., Fischer, W., and Bjorklund, A. (1989). NGF receptor reexpression and NGF-mediated cholinergic neuronal hypertrophy in the damaged adult neostriatum. Neuron *2*, 1177–1184.

Gardiner, K., Fortna, A., Bechtel, L., and Davisson, M.T. (2003). Mouse models of Down syndrome: how useful can they be? Comparison of the gene content of human chromosome 21 with orthologous mouse genomic regions. Gene *318*, 137–147.

Goate, A., Chartier-Harlin, M.C., Mullan, M., Brown, J., Crawford, F., Fidani, L., Giuffra, L., Haynes, A., Irving, N., James, L., et al. (1991). Segregation of a missense mutation in the amyloid precursor protein gene with familial Alzheimer's disease. Nature *349*, 704–706.

Golde, T.E., Estus, S., Usiak, M., Younkin, L.H., and Younkin, S.G. (1990). Expression of beta amyloid protein precursor mRNAs: recognition of a novel alternatively spliced form and quantitation in Alzheimer's disease using PCR. Neuron *4*, 253–267.

Goldstein, L.S. (2003). Do disorders of movement cause movement disorders and dementia? Neuron *40*, 415–425.

Gunawardena, S., and Goldstein, L.S. (2001). Disruption of axonal transport and neuronal viability by amyloid precursor protein mutations in *Drosophila*. Neuron *32*, 389–401.

Hodes, M.E., Woodward, K., Spinner, N.B., Emanuel, B.S., Enrico-Simon, A., Kamholz, J., Stambolian, D., Zackai, E.H., Pratt, V.M., Thomas, I.T., et al. (2000). Additional copies of the proteolipid protein gene causing Pelizaeus-Merzbacher disease arise by separate integration into the X chromosome. Am. J. Hum. Genet. *67*, 14–22.

Hof, P., Young, W.G., Bloom, E.F., Belichenko, P.V., and Celio, M.R. (2000). Comparative Cytoarchitectonic Atlas of the C57BL/6 and 129/SV Mouse Brains (New York: Elsevier).

Holtzman, D.M., Kilbridge, J., Li, Y., Cunningham, E.T., Jr., Lenn, N.J., Clary, D.O., Reichardt, L.F., and Mobley, W.C. (1995). TrkA expression in the CNS: evidence for the existence of several novel NGF-responsive CNS neurons. J. Neurosci. *15*, 1567–1576.

Holtzman, D.M., Santucci, D., Kilbridge, J., Chua-Couzens, J., Fontana, D.J., Daniels, S.E., Johnson, R.M., Chen, K., Sun, Y., Carlson, E., et al. (1996). Developmental abnormalities and age-related neurodegeneration in a mouse model of Down syndrome. Proc. Natl. Acad. Sci. USA *93*, 13333–13338.

Howe, C.L., and Mobley, W.C. (2004). Signaling endosome hypothesis: A cellular mechanism for long distance communication. J. Neurobiol. *58*, 207–216.

Jaffar, S., Counts, S.E., Ma, S.Y., Dadko, E., Gordon, M.N., Morgan, D., and Mufson, E.J. (2001). Neuropathology of mice carrying mutant APP(swe) and/or PS1(M146L) transgenes: alterations in the p75(NTR) cholinergic basal forebrain septohippocampal pathway. Exp. Neurol. *170*, 227–243.

Jankowsky, J.L., Slunt, H.H., Gonzales, V., Jenkins, N.A., Copeland, N.G., and Borchelt, D.R. (2004). APP processing and amyloid deposition in mice haplo-insufficient for presenilin 1. Neurobiol. Aging *25*, 885–892.

Kiss, J., Shooter, E.M., and Patel, A.J. (1993). A low-affinity nerve growth factor receptor antibody is internalized and retrogradely transported selectively into cholinergic neurons of the rat basal forebrain. Neuroscience *57*, 297–305.

Kleschevnikov, A.M., Belichenko, P.V., Villar, A.J., Epstein, C.J., Malenka, R.C., and Mobley, W.C. (2004). Hippocampal long-term potentiation suppressed by increased inhibition in the Ts65Dn mouse, a genetic model of Down syndrome. J. Neurosci. *24*, 8153–8160.

Koh, S., and Loy, R. (1989). Localization and development of nerve growth factor-sensitive rat basal forebrain neurons and their afferent projections to hippocampus and neocortex. J. Neurosci. *9*, 2999–3018.

Korenberg, J.R., Chen, X.N., Schipper, R., Sun, Z., Gonsky, R., Gerwehr, S., Carpenter, N., Daumer, C., Dignan, P., Disteche, C., et al. (1994). Down syndrome phenotypes: the consequences of chromosomal imbalance. Proc. Natl. Acad. Sci. USA *91*, 4997–5001.

Lai, F., and Williams, R.S. (1989). A prospective study of Alzheimer disease in Down syndrome. Arch. Neurol. *46*, 849–853.

Lamb, B.T., Sisodia, S.S., Lawler, A.M., Slunt, H.H., Kitt, C.A., Kearns, W.G., Pearson, P.L., Price, D.L., and Gearhart, J.D. (1993). Introduction and expression of the 400 kilobase amyloid precursor protein gene in transgenic mice. Nat. Genet. *5*, 22–30.

Lamb, B.T., Call, L.M., Slunt, H.H., Bardel, K.A., Lawler, A.M., Eckman, C.B., Younkin, S.G., Holtz, G., Wagner, S.L., Price, D.L., et al. (1997). Altered metabolism of familial Alzheimer's disease-linked amyloid precursor protein variants in yeast artificial chromosome transgenic mice. Hum. Mol. Genet. *6*, 1535–1541.

Lemere, C.A., Blusztajn, J.K., Yamaguchi, H., Wisniewski, T., Saido, T.C., and Selkoe, D.J. (1996). Sequence of deposition of heterogeneous amyloid beta-peptides and APO E in Down syndrome: implications for initial events in amyloid plaque formation. Neurobiol. Dis. *3*, 16–32.

Lupski, J.R., de Oca-Luna, R.M., Slaugenhaupt, S., Pentao, L., Guzzetta, V., Trask, B.J., Saucedo-Cardenas, O., Barker, D.F., Killian, J.M., Garcia, C.A., et al. (1991). DNA duplication associated with Charcot-Marie-Tooth disease type 1A. Cell *66*, 219–232.

Mann, D.M., Yates, P.O., Marcyniuk, B., and Ravindra, C.R. (1985). Pathological evidence for neurotransmitter deficits in Down's syndrome of middle age. J. Ment. Defic. Res. *29*, 125–135.

Petanceska, S.S., Nagy, V., Frail, D., and Gandy, S. (2000). Ovariectomy and 17beta-estradiol modulate the levels of Alzheimer's amyloid beta peptides in brain. Neurology *54*, 2212–2217.

Pinnix, I., Musunuru, U., Tun, H., Sridharan, A., Golde, T., Eckman, C., Ziani-Cherif, C., Onstead, L., and Sambamurti, K. (2001). A novel gamma -secretase assay based on detection of the putative C-terminal fragment-gamma of amyloid beta protein precursor. J. Biol. Chem. *276*, 481–487.

Prasher, V.P., Farrer, M.J., Kessling, A.M., Fisher, E.M., West, R.J., Barber, P.C., and Butler, A.C. (1998). Molecular mapping of Alzheimer-type dementia in Down's syndrome. Ann. Neurol. *43*, 380–383.

Price, D.L., and Sisodia, S.S. (1998). Mutant genes in familial Alzheimer's disease and transgenic models. Annu. Rev. Neurosci. *21*, 479–505.

Rovelet-Lecrux, A., Hannequin, D., Raux, G., Le Meur, N., Laquerriere, A., Vital, A., Dumanchin, C., Feuillette, S., Brice, A., Vercelletto, M., et al. (2006). APP locus duplication causes autosomal dominant early-onset Alzheimer disease with cerebral amyloid angiopathy. Nat. Genet. *38*, 24–26.

Sago, H., Carlson, E.J., Smith, D.J., Kilbridge, J., Rubin, E.M., Mobley, W.C., Epstein, C.J., and Huang, T.T. (1998). Ts1Cje, a partial trisomy 16 mouse model for Down syndrome, exhibits learning and behavioral abnormalities. Proc. Natl. Acad. Sci. USA *95*, 6256–6261.

Salehi, A., Delcroix, J.D., and Mobley, W.C. (2003). Traffic at the intersection of neurotrophic factor signaling and neurodegeneration. Trends Neurosci. *26*, 73–80.

Salehi, A., Lucassen, P.J., Pool, C.W., Gonatas, N.K., Ravid, R., and Swaab, D.F. (1994). Decreased neuronal activity in the nucleus basalis of Meynert in Alzheimer's disease as suggested by the size of the Golgi apparatus. Neuroscience *59*, 871–880.

Sambamurti, K., Shioi, J., Anderson, J.P., Pappolla, M.A., and Robakis, N.K. (1992). Evidence for intracellular cleavage of the Alzheimer's amyloid precursor in PC12 cells. J. Neurosci. Res. *33*, 319–329.

Seet, L.F., and Hong, W. (2001). Endofin, an endosomal FYVE domain protein. J. Biol. Chem. *276*, 42445–42454.

Selkoe, D.J. (2002). Alzheimer's disease is a synaptic failure. Science *298*, 789–791.

Seo, H., and Isacson, O. (2005). Abnormal APP, cholinergic and cognitive function in Ts65Dn Down's model mice. Exp. Neurol. *193*, 469–480.

Singleton, A.B., Farrer, M., Johnson, J., Singleton, A., Hague, S., Kachergus, J., Hulihan, M., Peuralinna, T., Dutra, A., Nussbaum, R., et al. (2003). alpha-Synuclein locus triplication causes Parkinson's disease. Science *302*, 841.

Sofroniew, M.V., Cooper, J.D., Svendsen, C.N., Crossman, P., Ip, N.Y., Lindsay, R.M., Zafra, F., and Lindholm, D. (1993). Atrophy but not death of adult septal cholinergic neurons after ablation of target capacity to produce mRNAs for NGF, BDNF, and NT3. J. Neurosci. *13*, 5263–5276.

Sofroniew, M.V., Howe, C.L., and Mobley, W.C. (2001). Nerve growth factor signaling, neuroprotection, and neural repair. Annu. Rev. Neurosci. *24*, 1217–1281.

Stokin, G.B., Lillo, C., Falzone, T.L., Brusch, R.G., Rockenstein, E., Mount, S.L., Raman, R., Davies, P., Masliah, E., Williams, D.S., et al. (2005). Axonopathy and transport deficits early in the pathogenesis of Alzheimer's disease. Science *307*, 1282–1288.

Van Esch, H., Bauters, M., Ignatius, J., Jansen, M., Raynaud, M., Hollanders, K., Lugtenberg, D., Bienvenu, T., Jensen, L.R., Gecz, J., et al. (2005). Duplication of the MECP2 region is a frequent cause of severe mental retardation and progressive neurological symptoms in males. Am. J. Hum. Genet. *77*, 442–453.

Wessendorf, M.W. (1991). Fluoro-Gold: composition, and mechanism of uptake. Brain Res. *553*, 135–148.

Whitehouse, P.J., Price, D.L., Clark, A.W., Coyle, J.T., and DeLong, M.R. (1981). Alzheimer disease: evidence for selective loss of cholinergic neurons in the nucleus basalis. Ann. Neurol. *10*, 122–126.

Wisniewski, K.E., Dalton, A.J., McLachlan, C., Wen, G.Y., and Wisniewski, H.M. (1985). Alzheimer's disease in Down's syndrome: clinicopathologic studies. Neurology *35*, 957–961.

Wu, C., Lai, C.F., and Mobley, W.C. (2001). Nerve growth factor activates persistent Rap1 signaling in endosomes. J. Neurosci. *21*, 5406–5416.

Yamada, T., Sasaki, H., Dohura, K., Goto, I., and Sakaki, Y. (1989). Structure and expression of the alternatively-spliced forms of mRNA for the mouse homolog of Alzheimer's disease amyloid beta protein precursor. Biochem. Biophys. Res. Commun. *158*, 906–912.

Ye, H., Kuruvilla, R., Zweifel, L.S., and Ginty, D.D. (2003). Evidence in support of signaling endosome-based retrograde survival of sympathetic neurons. Neuron *39*, 57–68.

Yeo, T.T., Chua-Couzens, J., Butcher, L.L., Bredesen, D.E., Cooper, J.D., Valletta, J.S., Mobley, W.C., and Longo, F.M. (1997). Absence of p75NTR causes increased basal forebrain cholinergic neuron size, choline acetyltransferase activity, and target innervation. J. Neurosci. *17*, 7594–7605.

Zheng, H., Jiang, M., Trumbauer, M.E., Hopkins, R., Sirinathsinghji, D.J., Stevens, K.A., Conner, M.W., Slunt, H.H., Sisodia, S.S., Chen, H.Y., et al. (1996). Mice deficient for the amyloid precursor protein gene. Ann. N Y Acad. Sci. *777*, 421–426.

Zweifel, L.S., Kuruvilla, R., and Ginty, D.D. (2005). Functions and mechanisms of retrograde neurotrophin signalling. Nat. Rev. Neurosci. *6*, 615–625.